JOURNAL OF AIRCRAFT
Vol. 48, No. 3, May–June 2011

Engineering Notes

Effect of Slenderness Ratio on Free-to-Roll Wing Aerodynamics

N. T. Gresham,* Z. Wang,† and I. Gursul‡
University of Bath,
Bath, England BA2 7AY, United Kingdom

DOI: 10.2514/1.C031286

I. Introduction

MANNED fighter aircraft and unmanned combat air vehicles may require high angle-of-attack maneuvers where the roll dynamics become crucial. Small unmanned air vehicles (UAVs) and fixed-wing micro air vehicles often have separated flows [1,2]. These small vehicles fly at relatively high angles of attack and close to the stall conditions due to the poor lift. Vertical gusts might induce roll instabilities at high angles of attack. This possibility is suggested based on the recent experiments in which rectangular, elliptical, and Zimmerman planforms exhibited self-induced roll oscillations, even before the stall angle [3,4].

Most of the knowledge on the aerodynamics of free-to-roll wings is on slender delta wings [5–7], which exhibit well understood free-to-roll oscillations about a zero mean roll angle. Free-to-roll aerodynamics of delta wings with lower sweep angles (or higher aspect ratios) have been investigated in recent experiments [8–14]. The existence of equilibrium at nonzero roll angles was reported for sweep angles $\Lambda \leq 65°$. The roll asymmetries are demonstrated in Fig. 1a for a simple delta wing with sweep angle of $\Lambda = 55°$ (taken from [14]). The variation of the mean roll angle as a function of angle of attack shows that nonzero roll angles are observed until the wing stalls. Here, we use the term "stall" to describe the onset of the flow regime for which there is no flow reattachment, and hence the roll angle becomes zero. Previous work [12] confirms that the "stall angle of the free-to-roll wing" is near the stall angle of the fixed wing (at zero roll angle) at which the lift force is maximum. The stall of the free-to-roll wing is very sudden as the angle of attack is increased. In contrast, for a slender delta wing with sweep angle $\Lambda = 70°$, roll asymmetries mostly disappear, as shown in Fig. 1b.

Contour plots in Fig. 2 are adapted from the data in [14], which show the mean roll angle and the standard deviation of roll angle in the free-to-roll experiments. The variation of the angle of attack at which the vortex breakdown appears at the trailing edge of the wing, as well as the stall angle of attack at which the lift is maximum (for zero roll angle), is added from another source [15] (shown as dashed lines). It is seen in Fig. 2a that, for wings with low sweep angles, roll asymmetries appear when the vortex breakdown is over the wing and becomes maximum near the stall angle. The magnitude of the mean roll angle decreases with increasing sweep angle and almost disappears for the most slender wing. The stall of the free-to-roll wing also becomes more gradual with increasing sweep angle. Figure 2b shows that, in a certain range of sweep angles and near the stall, self-induced roll oscillations are possible.

In this Note, we extend our experiments to cropped delta wings with an initial leading-edge sweep angle of $\Lambda = 55°$, as shown in Fig. 3. We anticipate that the slenderness ratio, defined as the chord length divided by the span, may be important. It was shown [7] that if the distance from the vortex origin divided by the span is larger than two, the wing rock of aircraft configurations is likely. Similarly, this ratio may be important for the onset of the roll asymmetries for the nonslender free-to-roll wings. Table 1 lists the aspect ratio and slenderness ratio for the wings shown in Fig. 3. For comparison, we also added the simple delta wing with $\Lambda = 70°$ into our study.

II. Experimental Methods

Figure 3 shows the cropped wings studied. The relevant dimensions and other properties are listed in Table 1. For all wings, the span was kept the same ($b = 335.6$ mm). All wings were fabricated out of aluminum with sharp leading edges. The thickness was 3 mm, and a double 10° bevel was applied at the leading edges, while the trailing edge had a straight cut (square tip). The moment of inertia about the roll axis for each wing was calculated using CAD software. Wing models were attached to a free-to-roll sting, as detailed in [14]. No initial roll angle was imposed upon any of the wings. The high-speed section of the closed-return wind tunnel at the University of Bath was used for all the testing. The working section of the wind tunnel has dimensions of $2.13 \times 1.52 \times 2.70$ m. All the experiments in this study were conducted at a tunnel speed of 30 ms^{-1}, and the maximum blockage for the wind-tunnel models was approximately 3%. The Reynolds numbers (based on wing root chord length) are similar to flight conditions for UAVs operating at low/transitional Reynolds numbers.

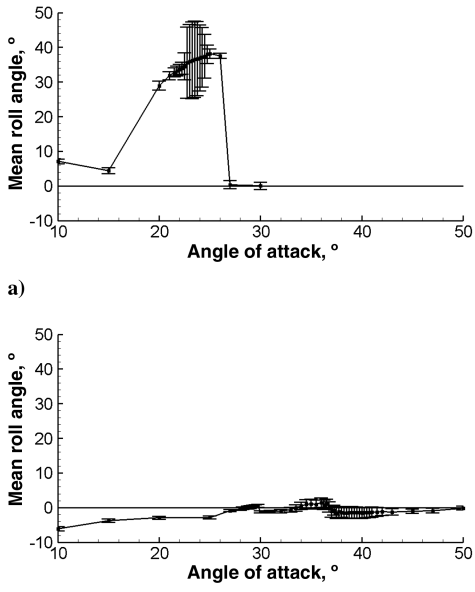

Fig. 1 Variation of mean roll angle as a function of angle of attack, with standard deviation as error bars, for a) $\Lambda = 55°$ and b) $\Lambda = 70°$, for simple delta wings.

Received 28 October 2010; revision received 14 February 2011; accepted for publication 15 February 2011. Copyright © 2011 by Ismet Gursul, Zhijin Wang, and Nick Gresham. Published by the American Institute of Aeronautics and Astronautics, Inc., with permission. Copies of this Note may be made for personal or internal use, on condition that the copier pay the $10.00 per-copy fee to the Copyright Clearance Center, Inc., 222 Rosewood Drive, Danvers, MA 01923; include the code 0021-8669/11 and $10.00 in correspondence with the CCC.

*Postgraduate Student, Department of Mechanical Engineering.
†Lecturer, Department of Mechanical Engineering.
‡Professor, Department of Mechanical Engineering. Associate Fellow AIAA.

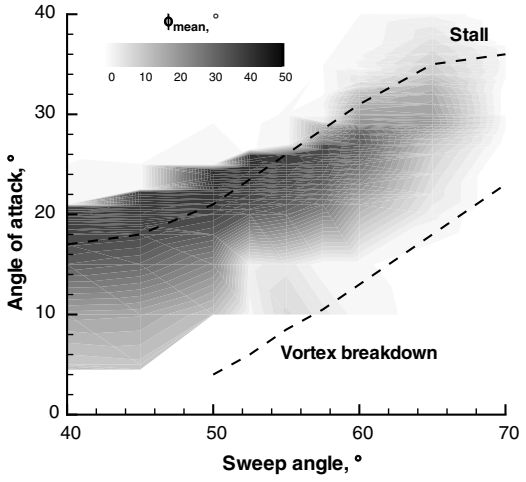

a)

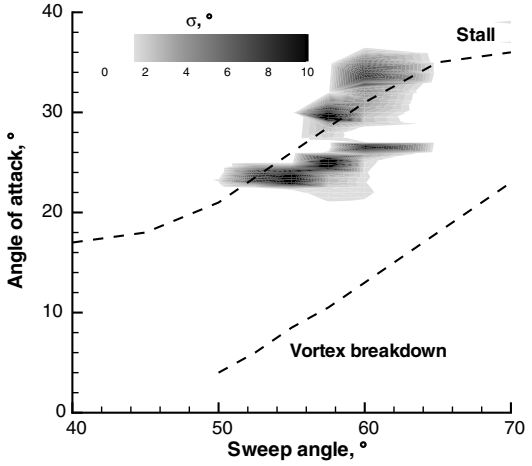

b)

Fig. 2 Contour plots showing variations of a) mean and b) standard deviation of roll angle for simple delta wings with different sweep angles.

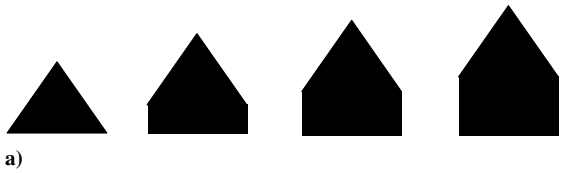

a)

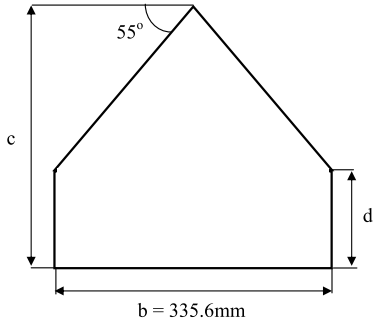

b)

Fig. 3 Wings tested in this study: a) schematic of wings with 55° sweep angle, and b) generic 55° sweep cropped delta wing planform, with main dimensions given in Table 1.

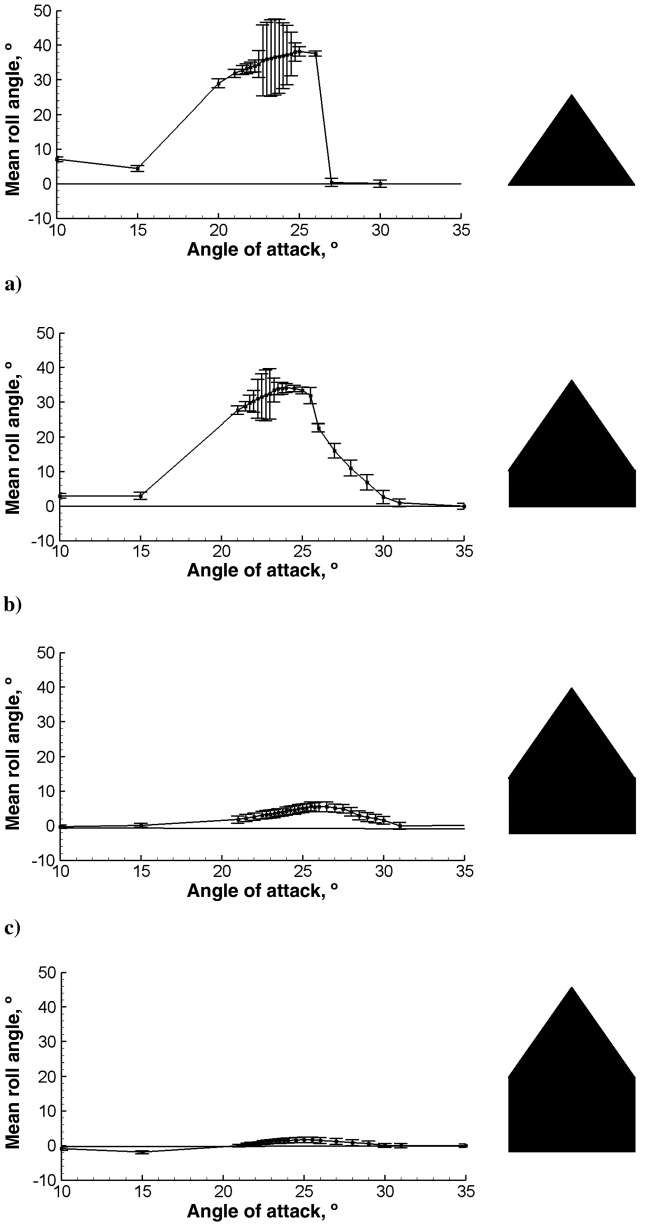

a) b) c) d)

Fig. 4 Variations of mean roll angle as a function of angle of attack with standard deviation as error bars and schematics of each wing (right) for a) simple delta wing and b–d) cropped delta wings with different cropped section lengths.

A dual 120 mJ neodymium-doped–yttrium-aluminum-garnet (Nd:YAG) digital particle-image-velocimetry (PIV) system was used to capture the velocity field, with seeding provided by a smoke machine placed in the low-speed section of the wind tunnel. The measurements were taken in crossflow planes at various chordwise locations, with multiple separate tests needed to cover the measurement domain. Details of these measurements are given in [16]. The measurement uncertainty for the velocity is estimated as 2% of the freestream velocity.

III. Results and Discussion

The time-averaged roll angle and the standard deviation of the roll angle (as error bars) are shown as a function of angle of attack for all wings with $\Lambda = 55°$ in Fig. 4. It is seen that the cropped delta wings may have very different free-to-roll dynamics, depending on the slenderness ratio of the wing. As the slenderness ratio increases (or

Table 1 Properties of wings tested

Leading-edge sweep, °	Aspect ratio, b^2/A	Slenderness ratio, c/b	c, mm	d, mm	t/c, %	I_{xx}, kgm^2	Re, $\rho U_\infty c/\mu$	Planform
55	2.80	0.71	239.7	0	1.25	1.3735×10^{-3}	410,000	Delta
55	1.28	1.01	339.7	100	0.88	3.6826×10^{-3}	581,000	Cropped delta
55	1.00	1.16	389.7	150	0.77	4.8295×10^{-3}	707,000	Cropped delta
55	0.83	1.31	439.7	200	0.68	5.9942×10^{-3}	839,000	Cropped delta
70	1.46	1.37	461.5	0	0.65	2.6582×10^{-3}	788,000	Delta

aspect ratio decreases), the nonzero mean roll angles diminish and, at the same time, roll oscillations disappear. Even the addition of a small cropped section, as in Fig. 4b, makes the stall more gradual and results in smaller magnitude of the roll oscillations. In Fig. 4c, for a slenderness ratio of 1.16, there are only slight roll asymmetries near the stall. For the slenderness ratio of 1.31, shown in Fig. 4d, the response is similar to that of the simple slender wing with $\Lambda = 70°$, shown in Fig. 1b. We have no evidence that the change in the moment of inertia has any correlation with the trim angles. The cropped delta wing with a slenderness ratio of 1.31 and the slender wing with a 70° sweep angle have similar slenderness ratios but very different moments of inertia (differing more than a factor of two), yet the trim angle responses are similar.

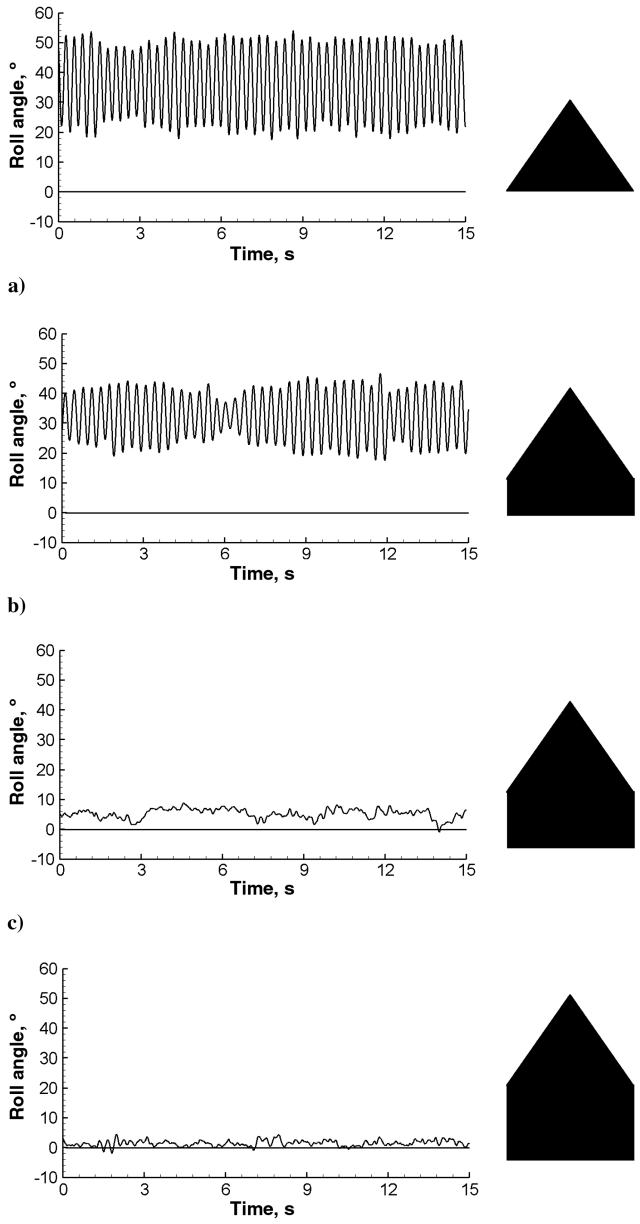

Fig. 5 Time histories of roll angle at angles of attack corresponding to maximum standard deviation ($\alpha = 23.25$, 22.75, 26, and 26°, respectively) and schematics of each wing (right) for a) simple delta wing and b–d) cropped delta wings with different cropped section lengths.

The corresponding time histories of the roll angle for each wing at the angle of attack with maximum standard deviation are shown in Fig. 5. For the slenderness ratio of 1.01, the roll oscillations exhibit some amplitude modulation. The Strouhal number of the oscillations ($Sr \cong 0.034$) is slightly larger compared with that of the simple delta wing ($Sr \cong 0.026$). With further increase in the slenderness ratio, the roll oscillations diminish.

With increasing slenderness ratio, cropped delta wings become more stable at zero roll angle. To understand the reasons behind this, we performed PIV measurements in crossflow planes. We studied the simple delta wing with $\Lambda = 55°$ (documented in [16]), the simple delta wing with $\Lambda = 70°$ (also documented in [16]), and the cropped delta wing with a slenderness ratio of 1.16. As a reminder, this cropped wing's free-to-roll response is a lot closer to that of the simple delta wing with $\Lambda = 70°$. For comparison, we fixed the angle of attack at $\alpha = 20°$ for the three wings.

These measurements showed that, as expected, the vortices are located close to the wing surface and more inboard for the $\Lambda = 55°$ simple delta wing, whereas for the slender wing with $\Lambda = 70°$, the vortices are located further away from the wing surface and more outboard [16]. Hence, we propose that the location of the vortices in the crossflow plane at zero roll angle may be a precursor for the roll stability or instability. For the cropped wing, we measured the crossflow velocity fields in two planes, as shown in Figs. 6a and 6b, the latter being the trailing edge, as shown in Fig. 6. At the end of the section with a sweep angle of 55° (Fig. 6a), the crossflow velocity and streamlines are very similar to those of the simple delta wing with the same sweep angle. The locations of the vortices are also very similar. At the trailing edge, the vortices are found to have moved away from the wing and outboard. In fact, the flowfield is more similar to that of a slender wing with $\Lambda = 70°$.

IV. Conclusions

Wind-tunnel experiments were conducted for various free-to-roll cropped delta wings, with the initial leading-edge sweep angle of $\Lambda = 55°$, as well as simple delta wings with sweep angles of $\Lambda = 55°$ and $\Lambda = 70°$. The two simple delta wings, representing the slender and nonslender delta wings, exhibit entirely different characteristics. The nonslender delta wing exhibits strong roll asymmetries, as well as roll oscillations, whereas the slender delta wing shows virtually no roll asymmetries and no roll oscillations. The response of the cropped delta wings falls in between these two cases. As the slenderness ratio (chord/span) increases, roll asymmetries decrease and roll oscillations disappear. For a slenderness ratio of approximately 1.3, there are no roll asymmetries.

For the nonslender simple delta wing, the vortices are located closer to the wing surface and more inboard compared with the slender simple delta wing. In contrast, for the slender delta wing, the vortices are more outboard and away from the surface, resulting in possibly one dominant vortex over the wing surface at a nonzero roll angle, which provides the restoring moment. Hence, it is hypothesized that the location of the vortices in the crossflow plane at

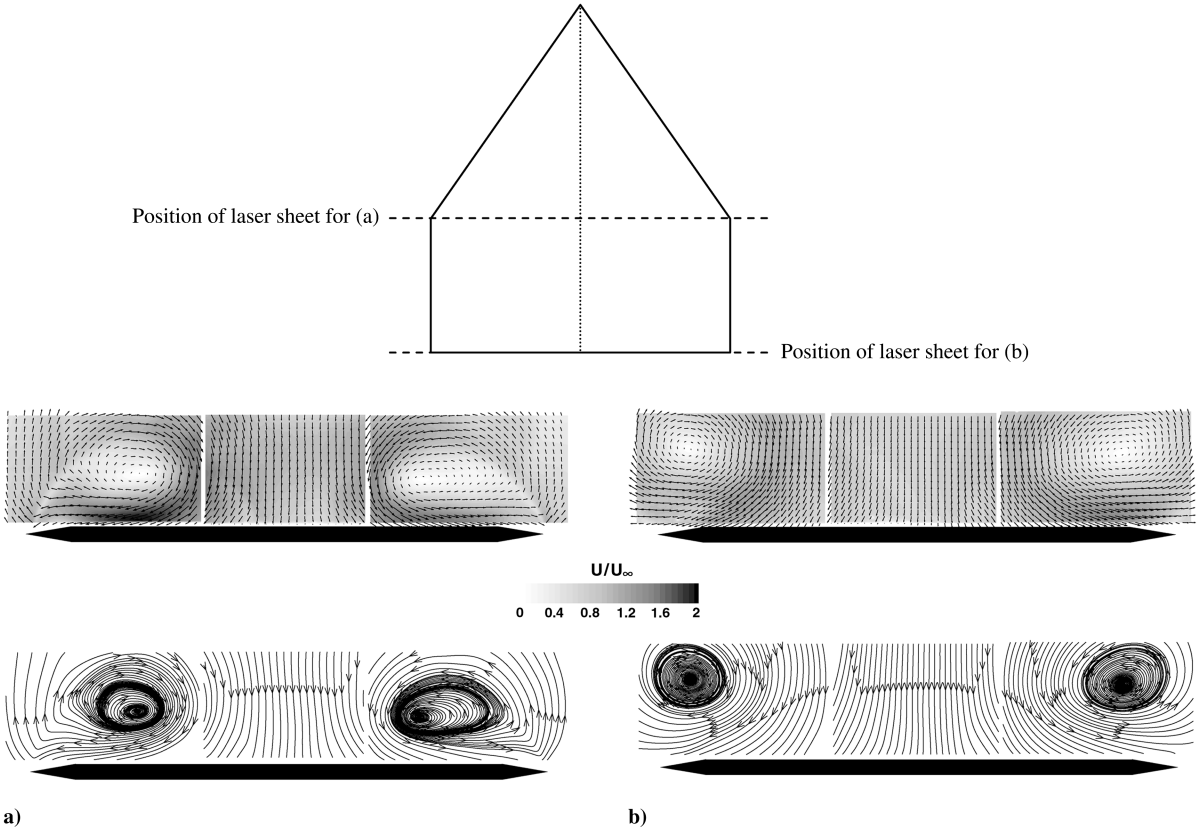

Fig. 6 Crossflow velocity and streamlines for stationary wing for a) $x/c = 39.5\%$ and b) trailing edge, at $\alpha = 20°$ and $\Phi = 0°$ for cropped delta wing with $\Lambda = 55°$, together with schematic of laser sheet locations (top).

the trailing edge at a zero roll angle may be a precursor for the roll instability. The cropped delta wing investigated exhibits a vortex topology similar to that of the slender wing at the trailing edge, which supports the hypothesis.

Acknowledgments

This work is sponsored by the U.S. Air Force (USAF) Office of Scientific Research, Air Force Material Command, USAF, under grant number FA8655-06-1-3058, and by the Research Councils United Kingdom Academic Fellowship in Unmanned Air Vehicles.

References

[1] Mueller, T. J., and DeLaurier, J. D., "Aerodynamics of Small Vehicles," *Annual Review of Fluid Mechanics*, Vol. 35, No. 1, Jan. 2003, pp. 89–111. doi:10.1146/annurev.fluid.35.101101.161102

[2] Gursul, I., "Vortex Flows on UAVs: Issues and Challenges," *The Aeronautical Journal*, Vol. 108, No. 1090, Dec. 2004, pp. 597–610.

[3] Gresham, N. T., Wang, Z., and Gursul, I., "Self-Induced Roll Oscillations of Nonslender Wings," *AIAA Journal*, Vol. 47, No. 3, March 2009, pp. 481–483. doi:10.2514/1.42511

[4] Gresham, N. T., Wang, Z., and Gursul, I., "Low Reynolds Number Aerodynamics of Free-to-Roll Low Aspect Ratio Wings," *Experiments in Fluids*, Vol. 49, No. 1, 2010, pp. 11–25. doi:10.1007/s00348-009-0726-2

[5] Levin, D., and Katz, J., "Dynamic Load Measurements with Delta Wings Undergoing Self-Induced Roll Oscillations," *Journal of Aircraft*, Vol. 21, No. 1, 1984, pp. 30–36. doi:10.2514/3.48218

[6] Arena, A. S., and Nelson, R. C., "Experimental Investigations on Limit Cycle Wing Rock of Slender Wings," *Journal of Aircraft*, Vol. 31, No. 5, 1994, pp. 1148–1155. doi:10.2514/3.46625

[7] Katz, J., "Wing/Vortex Interactions and Wing Rock," *Progress in Aerospace Sciences*, Vol. 35, No. 7, 1999, pp. 727–750. doi:10.1016/S0376-0421(99)00004-4

[8] Jenkins, J. E., Myatt, J. H., and Hanff, E. S., "Body-Axis Rolling Motion Critical States of a 65-Degree Delta Wing," *Journal of Aircraft*, Vol. 33, No. 2, 1996, pp. 268–278. doi:10.2514/3.46933

[9] Ueno, M., Matsuno, T., and Nakamura, Y., "Unsteady Aerodynamics of Rolling Thick Delta Wing with High Aspect Ratio," 16th AIAA Applied Aerodynamics Conference, Albuquerque, NM, AIAA Paper 1998-2520, June 1998.

[10] Matsuno, T., and Nakamura, Y., "Self-Induced Roll Oscillation of 45-Degree Delta Wings," 38th AIAA Aerospace Sciences Meeting and Exhibit, Reno, NV, AIAA Paper 2000-0655, Jan. 2000.

[11] Matsuno, T., Yokouchi, S., and Nakamura, Y., "The Effect of Leading-Edges Profile on Self-Induced Oscillations of 45-Degree Delta Wings," 18th Applied Aerodynamics Conference, Denver, CO, AIAA Paper 2000-4004, Aug. 2000.

[12] Gursul, I., Gordnier, R., and Visbal, M., "Unsteady Aerodynamics of Non-Slender Delta Wings," *Progress in Aerospace Sciences*, Vol. 41, No. 7, 2005, pp. 515–557. doi:10.1016/j.paerosci.2005.09.002

[13] McClain, A., Wang, Z-J., Vardaki, E., and Gursul, I., "Unsteady Aerodynamics of Free-to-Roll Non-Slender Delta Wings," 45th AIAA Aerospace Sciences Meeting and Exhibit, Reno, NV, AIAA Paper 2007-1074, Jan. 2007.

[14] Gresham, N. T., Wang, Z., and Gursul, I., "Vortex Dynamics of Free-to-Roll Slender and Nonslender Delta Wings," *Journal of Aircraft*, Vol. 47, No. 1, Jan.–Feb. 2010, pp. 292–302. doi:10.2514/1.45425

[15] Gursul, I., Wang, Z., and Vardaki, E., "Review of Flow Control Mechanisms of Leading-Edge Vortices," *Progress in Aerospace Sciences*, Vol. 43, Nos. 7–8, 2007, pp. 246–270. doi:10.1016/j.paerosci.2007.08.001

[16] Gresham, N. T., "Free-to-Roll Oscillations of Low Aspect Ratio Wings," Ph.D. Thesis, Univ. of Bath, Bath, England, U.K., Oct. 2010.